PERGAMON

Corrosion Science 42 (2000) 2085–2101

CORROSION SCIENCE

www.elsevier.com/locate/corsci

Characterization of Delhi iron pillar rust by X-ray diffraction, Fourier transform infrared spectroscopy and Mössbauer spectroscopy

R. Balasubramaniam[a,*], A.V. Ramesh Kumar[b]

[a]*Department of Materials and Metallurgical Engineering, Indian Institute of Technology, Kanpur 208 016, India*

[b]*Electrochemistry and Corrosion Division, Defense Materials, Stores Research and Development Establishment, Kanpur 208 013, India*

Received 19 February 1999; accepted 21 March 2000

Abstract

Rust samples obtained from the region just below the decorative bell capital of the Delhi iron pillar (DIP) have been analyzed by X-ray diffraction (XRD), Fourier transform infrared spectroscopy (FTIR) and Mössbauer spectroscopy. The identification of iron hydrogen phosphate hydrate in the crystalline form by XRD was unambiguous. Very weak diffraction from the oxyhydroxides/oxides of iron was observed indicating that these phases are most likely to be present in the amorphous form in the rust. The present XRD analysis of rust obtained from an inaccessible area of the DIP has also been compared with earlier analyses of DIP rust obtained from regions accessible to the public. FTIR indicated that the constituents of the scale were γ-, α-, δ-FeOOH, $Fe_{3-x}O_4$ and phosphate, and that the scale was hydrated. The unambiguous identification of the iron oxides/oxyhydroxides in the FTIR spectrum implied that they are present in the amorphous state, as XRD did not reveal these phases. The FTIR results have also been compared with earlier FTIR spectroscopic results of atmospheric rust formation. Mössbauer spectroscopy indicated that the rusts contained γ-FeOOH, superparamagnetic α-FeOOH, δ-FeOOH and magnetite, all in the amorphous form. The Mössbauer spectrum also confirmed that iron in the crystalline iron hydrogen phosphate hydrate, whose presence was confirmed by XRD, was in the ferric state indicating that it was a stable end corrosion product.

* Corresponding author.

0010-938X/00/$ - see front matter
PII: S0010-938X(00)00045-7

Keywords: Delhi iron pillar; Rust characterization; X-ray diffraction; Fourier transform infrared spectroscopy; Mössbauer spectroscopy; Phosphate; Amorphous iron oxyhydroxides

1. Introduction

The Delhi iron pillar (DIP) (Fig. 1) is a testimony to the high level of skill achieved by the ancient Indian iron smiths in the extraction and processing of iron. It has attracted the attention of archaeologists and corrosion technologists, as it has withstood corrosion for nearly 1600 years. Several theories, which have been proposed to explain its superior corrosion resistance, can be broadly classified into two categories [1–3]: the environmental and the material theories. The proponents of the environment theory state that the mild climate of Delhi is responsible for the corrosion resistance of the (DIP), while on the other hand, several investigators have stressed the importance of the material of construction as the primary cause for its corrosion resistance. These theories have been critically reviewed elsewhere [1–3]. The role of slag particles in enhancing the passivity in the material has also been mentioned earlier [2,3]. The precise reason for the corrosion resistance of the famous 1600-year-old DIP is not well understood. In order to glean insights into the nature of the passive film that forms on the DIP (which is responsible for its excellent resistance to atmospheric corrosion [3]), a detailed characterization study of the undisturbed rust from the region just below the decorative bell capital of the DIP was undertaken. The characterization of rust samples by X-ray diffraction (XRD), Fourier transform infrared spectroscopy (FTIR) and Mössbauer spectroscopy is the subject of the present communication.

The reason for utilizing several different characterization techniques must be emphasized. XRD analysis would provide information about phases that possess long range order and not about amorphous phases. Therefore, XRD analysis alone would not provide the complete picture of the rust's nature, especially if it contains amorphous matter. As several iron oxides/oxyhydroxides that form on iron during atmospheric corrosion can be amorphous in nature, these phases would not provide any diffraction peaks, and therefore, XRD is not the characterization technique that will reveal the presence of these amorphous phases in the rust. The characterization technique, which can reveal the different allotropic modifications of iron oxides and oxyhydroxides even if they are amorphous in nature, is FTIR. The results of FTIR coupled with that of Raman spectroscopy (which provides complementary information) should provide information about the various forms of iron oxides and oxyhydroxides present, but they will not provide any information whether the phases are amorphous or crystalline in nature, as both these techniques utilize radiation (infrared in FTIR spectroscopy and visible in Raman spectroscopy) for determining the molecular

vibration (due to bending and stretching of the bonds) between iron and oxygen [4]. As the molecular vibration in all known iron oxides and hydroxides are well characterized and available in the literature, comparison of the FTIR spectra from the DIP rust with standards would provide the exact nature of the phases of iron oxides and oxyhydroxides present. IR spectroscopy has been successfully utilized

Fig. 1. The Delhi iron pillar before the construction of the iron grill cage around the stone platform.

to identify iron oxide/oxyhydroxide phases under atmospheric corrosion [5,6] and aqueous corrosion [7] conditions.

Mössbauer spectroscopy can be used to obtain further insights on the structural (i.e. amorphous or crystalline) and chemical aspects of the rusts. Mössbauer spectroscopy is a powerful tool to understand the amorphous versus crystallinity controversy in the case of oxides/oxyhydroxides [8]. In case the phase that constitutes the rust is crystalline, it would lead to alignment of magnetic fields in the individual grains of the phase and provide a characteristic hyperfine splitting with characteristic magnetic fields. For example, in the case of crystalline magnetite, two sextets (10-line pattern) are to be expected in the Mössbauer spectrum at ambient temperatures. However, in case this phase is amorphous, the magnetic fields will not be aligned in the individual grains and this would result in collapse of magnetic fields or as a result of which a doublet would be obtained instead of a sextet [8–10]. A collapsed sextet would indicate the fine nanocrystalline nature of magnetite. Therefore, Mössbauer spectroscopy can be advantageously utilized to probe the crystal nature (i.e. amorphous or crystalline) of the phase. The use of Mössbauer spectroscopy for elucidation of the chemical nature of corrosion products is also well established [8,11–13]. Another advantage of utilizing Mössbauer spectroscopy is that the asymmetry in any peak of central doublet indicates the contribution due to some other species (phase). For example, Fe^{2+} ions show high positive value for isomer shift and quadrupole splitting resulting in asymmetry in the central doublet in which a higher intense first peak (from left) is obtained. The second peak of ferrous doublet will be in the more positive region of the spectrum [14].

2. Experimental

Rust samples were collected using a plastic scraper from several different locations in the region just below the decorative bell capital (Fig. 2(a)). Observation of the same region, nearly a year after the samples were collected (Fig. 2(b)), did not reveal any evidence for rust removal, thereby indicating that the passive film is self-healing. This is the region where the rust layer on the exposed surface of the pillar is maximum [15] and therefore, this allowed the collection of a significant amount of rust suitable for characterization by several techniques. Moreover, this is the region where the rust is the oldest as this portion of the pillar is inaccessible to the public. A portion of the rust sample collected from each location was first ground into fine powder and mounted in between two thin polymer foils. A part of the same ground powder was also analyzed using FTIR. The polymer foil containing the DIP rust was used for Mössbauer spectroscopic analysis of the phases present.

The polymer foils were mounted in a diffractometer such that the flat foil was placed horizontally and the incident beam could sample the specimen through the whole range of 2θ studied. Several diffraction patterns were obtained using Cu K_α radiation at different scan speeds and scanning angle steps. The present paper

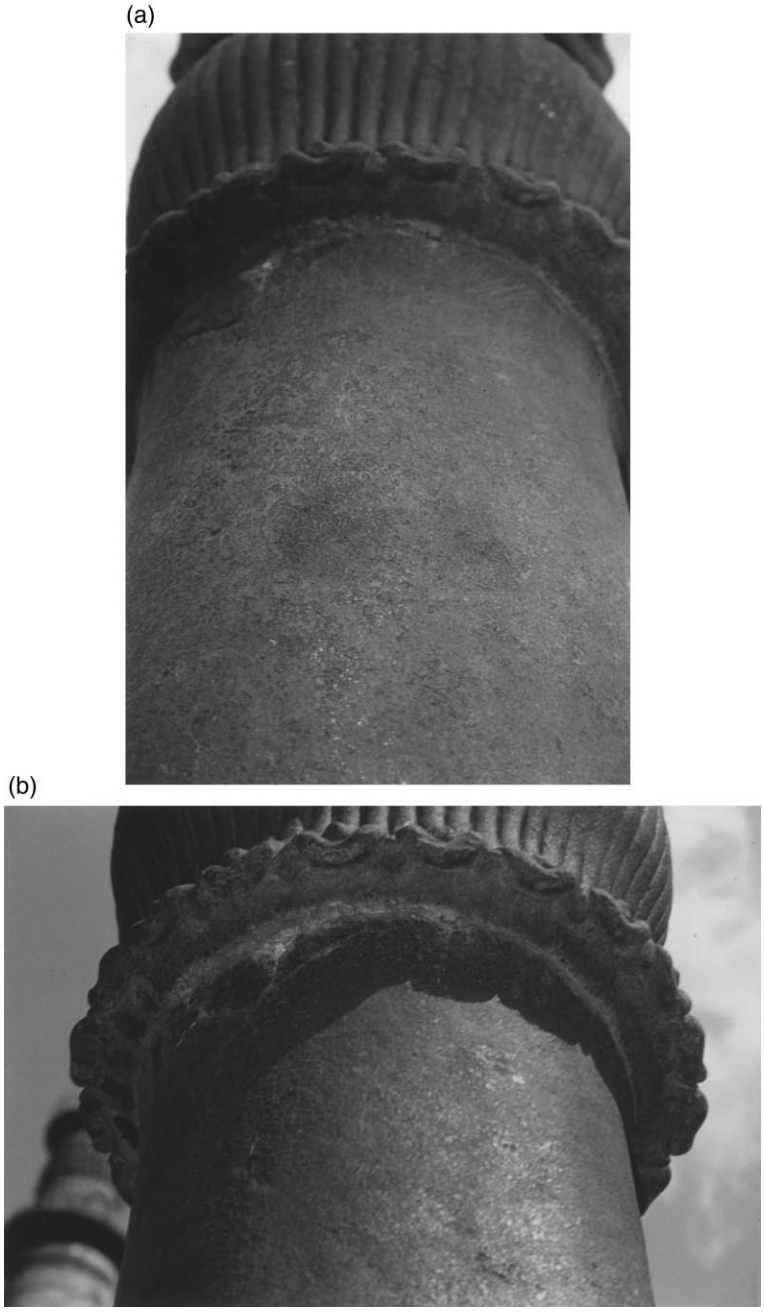

Fig. 2. (a) Location from below the decorative bell capital from where the rust samples were collected and (b) same location photographed after nearly a year indicating that the rust is self-healing.

reports the diffraction pattern taken at a scan rate of 3° per min (i.e. 0.05° per s), with the scan being conducted between $2\theta = 10$–$80°$ in steps of 0.05°.

A small portion of the rust was finely ground and then pressed (in vacuum) in the form of a disc using spectroscopically pure dry KBr. The FTIR spectrum was recorded at room temperature using a Nicolet Magna 750 Series 2, USA FTIR system.

In order to study the rust by Mössbauer spectroscopy, the polymer foils were mounted on a sample holder of a Mössbauer spectrometer in transmission geometry. The spectrometer controller model was S-600 of Austin Science Associates, USA with linear motor of ASA, USA which was coupled with a Norland Ortec Multichannel analyzer and proportional counter (Kr at 1 atm and 3% CO_2) manufactured by Ranger Corporation, USA and these were used to count the 14.4 KeV γ-ray. The source used was 400 MBq ^{57}Co source in Palladium matrix (Amersham, UK). The Mössbauer spectrum was recorded in a fly back mode at room temperature in 1024 channels, which gives a single spectrum. The Mössbauer data was fitted to Lorentzian approximation using mm/sirus v.2.7 Mössbauer data handling program [16]. The Mössbauer parameters reported are with respect to α-Fe standard.

3. Results and discussion

3.1. X-ray diffraction

3.1.1. Phase identification

The complete diffraction pattern obtained from the rust is presented in Fig. 3. The results from the second rust sample were identical. The XRD data were analyzed with the corrosion products of iron, phosphorus, lead, chromium, nickel, copper, and tin using JCPDS diffraction files [17]. The JCPDS data of oxides and oxyhydroxides of iron were compared carefully. The angles and the relative intensities (after subtracting the background radiation) are provided in Table 1. The peaks could only be unambiguously identified with iron hydrogen phosphates. The diffraction peaks were carefully compared with the standard for iron

Table 1
XRD analysis of Delhi iron pillar rust using Cu K_α radiation

2θ (expt) (°)	I/I_0 (expt) (%)	phase	2θ (standard) (°)	I/I_0 (standard) (%)
12.75	25	$FeH_3P_2O_8{\cdot}4H_2O$	12.249	100
15.40	100	$FeH_3P_2O_8{\cdot}4H_2O$	15.424	44
16.90	15	$FeH_3P_2O_8{\cdot}4H_2O$	16.939	38
24.15	22	$FeH_3P_2O_8{\cdot}4H_2O$	24.689	19
			25.848	18
26.90	6	$FeH_3P_2O_8{\cdot}4H_2O$	26.848	45

phosphate ($FePO_4{\cdot}2H_2O$ — file number 33-0667) and several other iron hydrogen phosphate hydrates ($FeH_3P_2O_8{\cdot}4H_2O$ — file number 45-0500, $FeH_6P_3O_9{\cdot}H_2O$ — file number 31-0623, $FeH_2P_3O_{10}{\cdot}(3/2)H_2O$ — file number 28-0486 and $FeH_3P_2O_6{\cdot}3H_2O$ — file number 31-0624) [17]. All the peaks could be identified with the phase $FeH_3P_2O_8{\cdot}4H_2O$. The 2θ values and corresponding intensity of the peaks from the standard diffraction file of $FeH_3P_2O_8{\cdot}4H_2O$ are also provided in Table 1. It is seen that the high intensity peak of the phase $FeH_3P_2O_8{\cdot}4H_2O$ appears as a significant peak at 2θ of 12.75°. The experimental peak occurring at 2θ of 15.40° is again a significant peak of the phase $FeH_3P_2O_8{\cdot}4H_2O$. The possible reasons for the experimentally determined peak at 15.40° being the highest intensity peak rather than the peak at 12.75° are (a) different degrees of hydration, (b) slight differences in composition, and (c) orientation effects in the DIP rust sample as compared to the standard. Contribution to the 100% experimental peak (at 2θ of 15.40°) due to diffraction from other planes is also a possibility as the standard pattern shows the presence of three diffraction peaks clustered very near to this angle. A similar situation is obtained for the diffraction peak occurring at 2θ of 24.15°, as there are two significant peaks (of theoretical intensities 19 and 18%) of the phase $FeH_3P_2O_8{\cdot}4H_2O$ occurring near this diffraction peak (Table 1). Therefore, there is no ambiguity in the identification of the iron hydrogen phosphate hydrate phase ($FeH_3P_2O_8{\cdot}4H_2O$) in the DIP rust as the experimentally

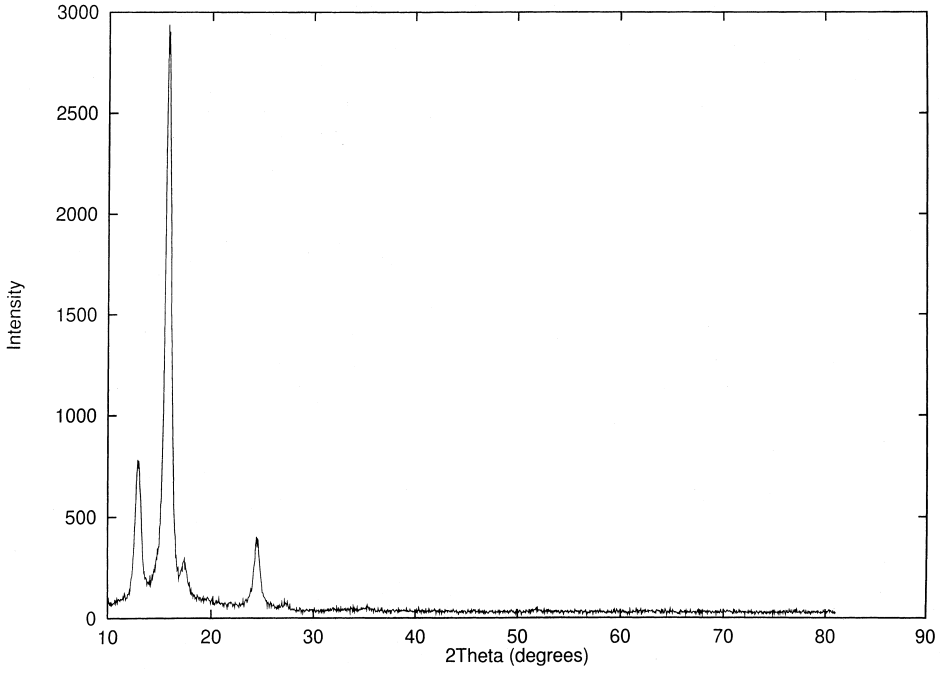

Fig. 3. X-ray diffraction pattern of the DIP rust showing the intensities in the region $2\theta = 10 - 80°$.

obtained relative intensities can also be matched to the standard JCPDS diffraction data of this phase.

As the rust obtained is very old, it is not surprising that the stable crystalline form of iron hydrogen phosphate hydrate [18] was identified. However, it should be borne in mind that the presence of the precursor to this phase, i.e. $Fe_3(PO_4)_2$ in the rust could not be ruled out as it is amorphous [18] in nature and would not have provided diffraction peaks. Its relative amount is not important as it is the precursor to the much more stable crystalline form of iron hydrogen phosphate hydrate, which has been unambiguously identified in the rust by XRD.

The presence of $FeH_3P_2O_8{\cdot}4H_2O$ is also theoretically favored as it is composed of $FePO_4$ and H_3PO_4, whose standard free energies for formation is extremely negative at room temperature. At 298.15 K and 1 bar pressure, the standard free energy of formation of $FePO_4{\cdot}2H_2O$ is -1657.5 kJ/mol, while that for crystalline H_3PO_4 is -1119.2 kJ/mol [19]. In comparison, the standard free energies of formation of the oxides and oxyhydroxides of iron are much higher [19]. On the topic of thermodynamics, it is interesting to note the experimental result of Urasova et al. [20] who found that phosphate is stable even at P concentration as low as 0.24 wt% in the Fe-P-O system. Therefore, the identification of iron hydrogen phosphate hydrate is reliable as the laws of thermodynamics are exact and conclusions based on thermodynamics are sound and reliable.

From the above analysis, it would apparently appear that the rust of the iron pillar is composed of only iron phosphates. This may not be true as very careful analysis of the XRD pattern revealed weak peak(s) in the region of $2\theta = 30 - 35^\circ$ (Fig. 4). When the diffraction data of the several oxides and oxyhydroxides of iron were analyzed, it was noticed that the maximum intensity peaks in the case of several iron oxides and oxyhydroxides are concentrated in the 2θ range between 30 and 35°. It, therefore, appears from the very weak diffraction intensities obtained in this range that there should be a very small amount of crystalline iron oxides or oxyhydroxides present in the rust.

3.1.2. Comparison with earlier XRD studies

Earlier XRD studies of rusts from the DIP are summarized below in order to compare the present results with them. The rust samples that were obtained in the present case were taken from the surface of the pillar just below the decorative bell capital and this rust must be the oldest rust on the pillar. Moreover, this rust has been undisturbed because this location of the pillar is inaccessible to the public. Therefore, this important aspect must be borne in mind while viewing the earlier rust analyses as all of them were conducted on rusts obtained from the lower regions of the pillar. The rust forming in the lower regions cannot be in the undisturbed condition because of the custom of the visitors who try to encircle their arms around the pillar with their backs against the pillar in the belief that if such an act can be successfully completed, it brings good luck.

A minute sample of the rust scraped from the area about 5 feet from the ground was found essentially amorphous and contained clayey and siliceous matter [21]. X-ray fluorescent analysis of the same rust confirmed that there was

no free iron present in the rust. Based on these results, Bardgett and Stanners [21] proposed that the coating might have risen from repeated handling. This conclusion is not surprising as the rust sample was taken from the location where contact with humans was frequent. Ghosh [22] analyzed the rust obtained from the buried underground portion of the DIP and from the portion above the ground. He found that both the samples were contaminated with sandy and clayey matter. The rust samples were separated with a magnet and it was found that the DIP underground rusts contained 99.0% of magnetic matter, while the rust sample from the exposed area contained 65.7–80.1% of magnetic matter. X-ray diffraction analysis of the rusts (conducted at Bern University [22]) revealed that the magnetic portion contained γ-FeOOH (lepidocrocite), α-FeOOH (goethite) and $Fe_{3-x}O_4$ (magnetite), while the non-magnetic portion contained γ-FeOOH and quartz. Interestingly, although the presence of α-Fe_2O_3 (maghmite) was not confirmed directly, it was opined that there might be some α-Fe_2O_3 present based on the asymmetry of diffraction lines of $Fe_{3-x}O_4$ [22]. It is well known that magnetite formation is favored in restricted oxygen environments, such as soil burial conditions. Therefore, the higher proportion of magnetic matter in the underground rust must be due to a higher magnetite content in them.

The identification of the oxides/oxyhydroxides in the rust samples taken from above the ground are indicative of the state of the rust in the region where the pillar comes into contact with humans. This is not the stable rust layer present on

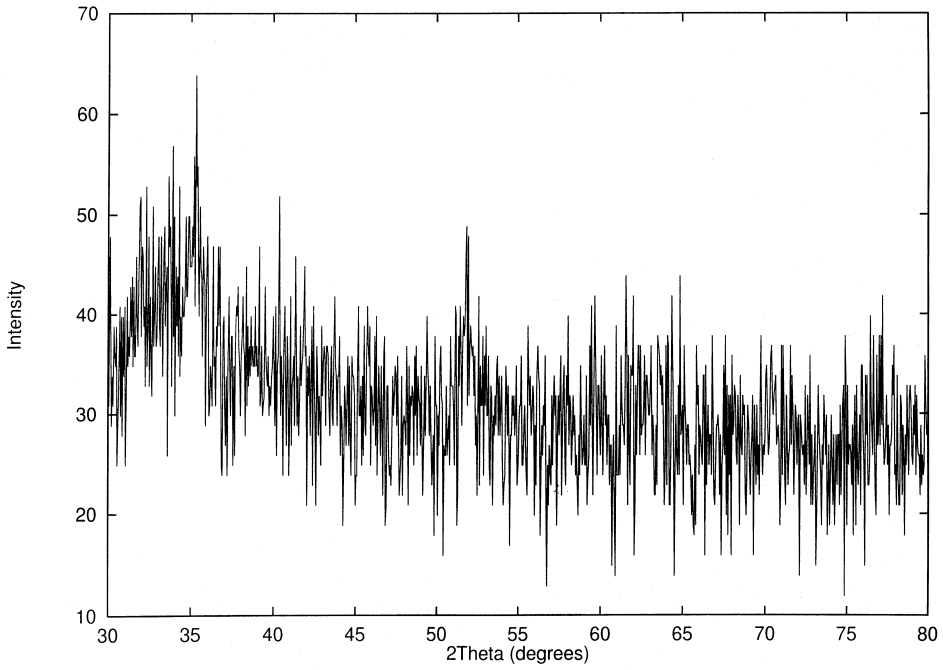

Fig. 4. X-ray diffraction pattern of the DIP rust showing the intensities in the region $2\theta = 30 - 80^{\circ}$.

the pillar. However, the above observation provide information about the rust layer in the region that was in human contact. Interestingly, a sample was cut from the bottom exposed region of the pillar for metallographic analysis [22] and the rust formed on this freshly exposed surface after 1.5 years of exposure was studied by XRD by Lahiri et al. [23]. They identified γ-FeOOH (lepidocrocite) and α-FeOOH (goethite) in the rust, with the major phase being γ-FeOOH (lepidocrocite) based on the diffraction intensities. While the above studies provide information about the state of the rust in the ground level region of the pillar, the XRD results provided in the present study provides information about the state of the stable oldest rust on the pillar. Nevertheless, the information from the above studies can be utilized to construct the sequence of events leading to the formation of the protective passive film on the DIP [24].

3.2. Fourier transform infrared spectroscopy

It is established that IR spectroscopy can be utilized to understand the process of rusting of steels. Misawa et al. [5,6] studied the mechanism of atmospheric rusting and the protective amorphous rust on low allow steel by using IR absorption spectroscopy. It has been pointed out by them that the absorption band at higher wavenumber region is due to OH stretching and at lower wavenumber is because of Fe–O lattice vibration. Misawa et al. [5,6] attributed the following peaks as key absorption bands: 890 cm^{-1} for α-FeOOH, 1020 cm^{-1} for γ-FeOOH, 580 cm^{-1} for magnetite and 470 cm^{-1} for δ-FeOOH. Ishii et al. [25] also confirmed that the Fe–O stretching vibration in $Fe_{3-x}O_4$ corresponds to a wave number 570 cm^{-1}. Moreover, they also showed that if this peak is sharp, it indicates the purity level and the prevalence of very small amount of defects [25]. Raman et al. [26] applied IR absorption spectroscopy to the study of atmospheric rust and they have provided standard spectra for different phases. Music et al. [7] used Fourier transform infrared spectroscopy for the analysis of rust formed by corrosion of steel in aqueous solutions. Yamashita et al. [27] studied the rust layer, formed on weathering steel for a quarter of a century in an industrial region, by IR absorption spectroscopy where the bands obtained were relatively broad.

3.2.1. Phase identification

The FTIR spectrum obtained from one DIP rust sample is provided in Fig. 5. The spectrum obtained from another rust sample was identical and therefore is not presented. In order to precisely identify the peaks that are due to KBr and other IR active molecules (i.e. control specimen) present in the atmosphere, the spectrum was recorded at ambient room atmosphere and not in an inert atmosphere. The FTIR spectrum of the control sample is provided in Fig. 6. The following discussion will address the identification of phases present in the DIP rust based on the two spectra presented above.

On comparing the DIP rust and control spectra, it is clear that the peaks that occur in the control sample in the region around 1500, 2920 and 2850 cm^{-1} arise

from C=O and O–H stretchings [4,28] which are present in the atmosphere. When these peaks are eliminated from analysis in the DIP rust FTIR spectrum, only certain other significant peaks require to be identified. The broad band seen in the region 3000–3500 cm^{-1} is due to hydration of the rust. It is known that O–H stretching leads to a strong peak between 3000 and 3700 cm^{-1}, while O–H bending to a medium band between 1200 and 1500 cm^{-1} [4,28]. Therefore, this implies hydration of corrosion product(s) in the DIP rust.

It can be noted from Fig. 5 that the presence of γ-FeOOH, α-FeOOH and δ-FeOOH is confirmed by the appearance of peaks at 1020 cm^{-1} (γ-FeOOH), 890 cm^{-1} (α-FeOOH) and 470 cm^{-1} (δ-FeOOH) [5,6]. The DIP rust FTIR spectrum also reveals that δ-FeOOH is the major component of the rust as the peak is relatively intense compared to the others. This phase forms due to catalytic action of elements like Cu, P, and Ni that are added for weathering resistance [5]. Interestingly, the peak due to magnetite ($Fe_{3-x}O_4$) was present at 580 cm^{-1}. This indicates the relatively more protective nature of the DIP rust. It is known that magnetite formed during atmospheric corrosion will be non-stoichiometric and as the non-stoichiometry increases, a rapid decrease in electrical conductivity is observed in turn due to localization of electrons to regions encompassing available octahedral Fe pairs [29]. The present FTIR results of the DIP rust are compared

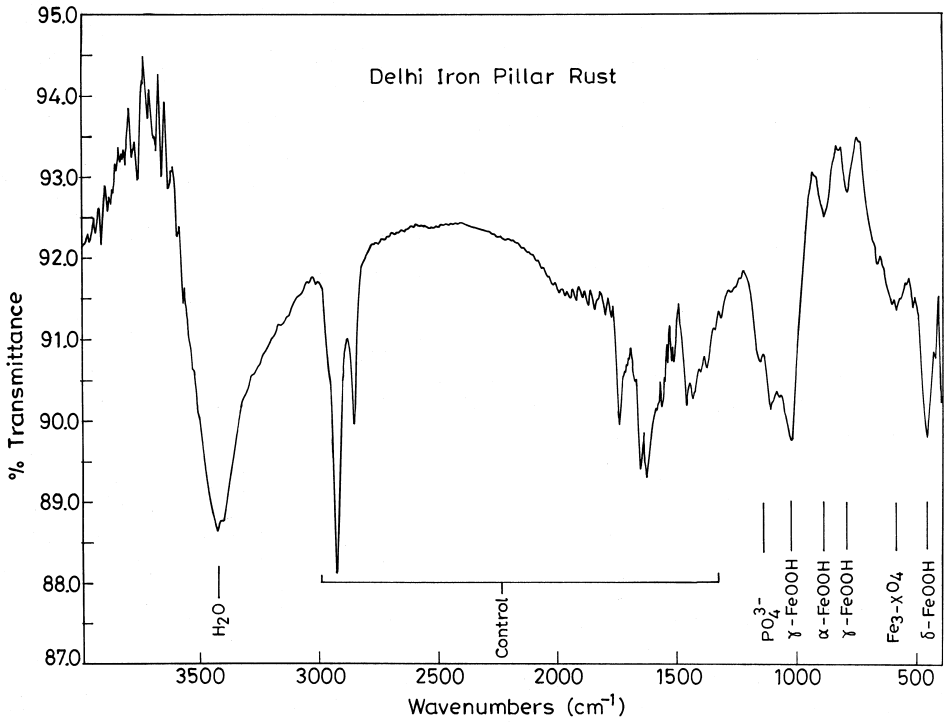

Fig. 5. FTIR spectrum from the DIP rust.

with that of the rust on a Gupta-period corrosion resistant iron clamp, which was analyzed earlier [30]. The FTIR spectrum from the Eran rust (Figure 3 of Ref. [30]) revealed characteristic peaks due to γ-, α- and δ-FeOOH. Moreover, the existence of magnetite (that was likely doped with P ions) in the crystalline form was identified in contrast to the amorphous nature of magnetite in DIP's rust. In order to appreciate this difference, it is important to keep in mind the environmental conditions in which the Eran rust and DIP rust were obtained. The Eran iron clamp was removed from a stone block where it was buried inside. The stone block was part of the oldest temple at Eran which was built by Chandragupta II Vikramaditya [31], the *Chandra* mentioned in the DIP's oldest Sanskrit inscription [32]. The major difference between the Eran and DIP rust was that the former was obtained from a restricted environment in a stone block (thereby implying restricted oxygen supply to the surface of the iron clamp) whereas, the rust on the DIP was obtained from a surface exposed to the atmosphere. Under the condition of restricted oxygen supply, it is well established that the rust that forms on iron is magnetite. Therefore, it is not surprising that magnetite was obtained in the crystalline form in the Eran iron clamp. On the other hand, the DIP rust is exposed to the environment where it undergoes constant wetting and drying cycles and in such a case, it is observed that the

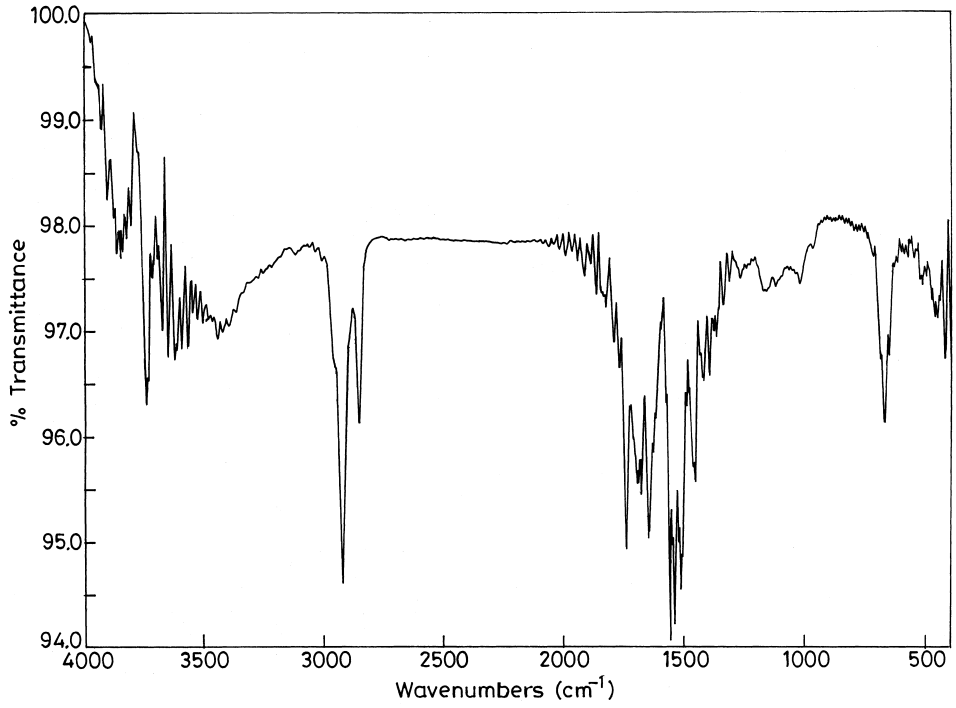

Fig. 6. FTIR spectrum from control specimen.

magnetite in the rust is amorphous in nature. The reason for the presence of magnetite in the amorphous form has been addressed elsewhere [24].

An interesting aspect that was found from the FTIR spectrum was that there was a distinct band resulting from the presence of some phosphate phase(s) in the region 1250–900 cm^{-1} [4]. The wavenumber for ionic phosphate is 1030–1120 cm^{-1}, while for covalent phosphate the band should occur at 920–1050 cm^{-1} and for P=O bonds, the spectra occur at 1200–1250 cm^{-1} [4,28]. Although it is difficult to tell whether the ionic phosphate that is providing the signal in the spectra is due to H_3PO_4 or $FePO_4$ or both, FTIR spectroscopy, nevertheless, firmly proves the existence of phosphates in the DIP rust.

3.3. Mössbauer spectroscopy

Mössbauer spectra of the rust samples obtained from two different locations in the region just below the decorative bell capital of the DIP are presented in Figs. 7 and 8. The continuous line in the spectra in these figures are computer fitted. The dots are experimental points. On comparing the Mössbauer spectra in Figs. 7 and 8, it is evident that both the rust samples exhibit a similar nature because both exhibit a collapsed sextet and a central doublet. As the results from two rust samples (taken from different locations in the top regions of the pillar) were identical, the validity of the characterization is established. Calculation of Mössbauer parameters showed a low value for isomer shift (IS) i.e. 0.08 mm/s in the first sample and 0.15 mm/s in the second sample. However, quadrupole splitting (QS) values (i.e. 0.55 mm/s and 0.58 mm/s for samples 1 and 2,

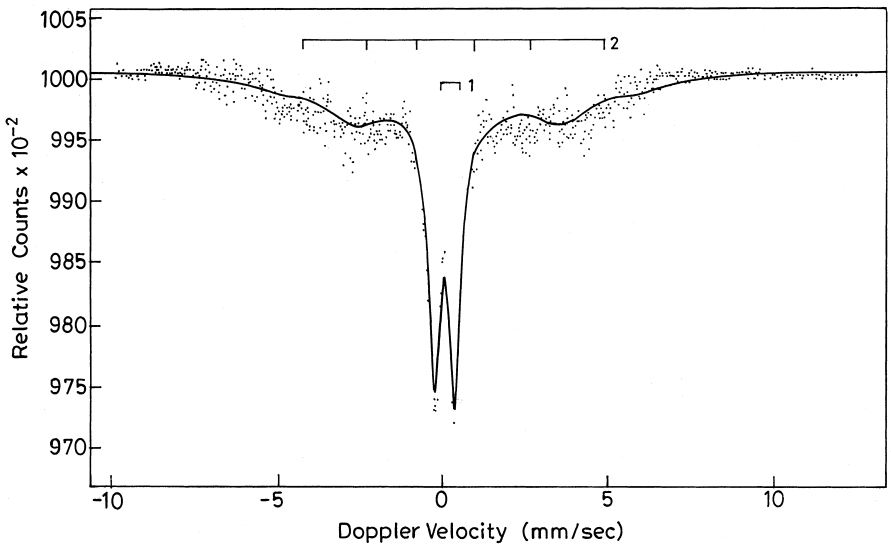

Fig. 7. Mössbauer spectrum obtained from the first DIP rust sample.

respectively) matched with literature values reported for oxyhydroxides [12–14]. Ferric phosphate shows an IS value of about 0.30 mm/s [33]. The deviation from the standard reported valued of isomer shifts could be due to the modified environment of the species responsible for the doublet. FTIR showed characteristic peaks for γ-FeOOH, α-FeOOH and δ-FeOOH indicating that they were in the pure form. However, a broad band was obtained for magnetite and phosphate indicating that they either exist in a different form or are incorporated with ions [26]. The sextet was tried to be fit for α-FeOOH with a magnetic field of 313 KOe (IS = 0.40 mm/s and QS = 0.09 mm/s [34]) but good fitting could not be obtained. Therefore, the collapsed sextet is due to magnetite that is in fine nanocrystalline or amorphous form [35].

In order to understand the nature of the rust, the Mössbauer spectrum obtained from the DIP rust from one location was analyzed in detail (Fig. 7). The same rust was earlier analyzed by XRD and FTIR. The central doublet showed a high value of 0.58 mm/s and 0.72 mm/s for full width at half maxima for individual peaks from left to right, respectively. A similar high value was also observed in the second sample. From these observations, it is clear that many species are being depicted as the central doublet in the Mössbauer spectrum. Singh et al. [8] showed at room temperature that γ-FeOOH, α-FeOOH and $Fe_{3-x}O_4$ (all exhibiting superparamagnetic behavior) existed in rust samples on weathering steels and only a central doublet was obtained at room temperature. Secondly, if only γ-FeOOH, δ-FeOOH and superparamagnetic α-FeOOH were present, it should have shifted the central doublet to more positive velocity region resulting in an IS value of about 0.40 mm/s. As the IS obtained in the DIP rust samples

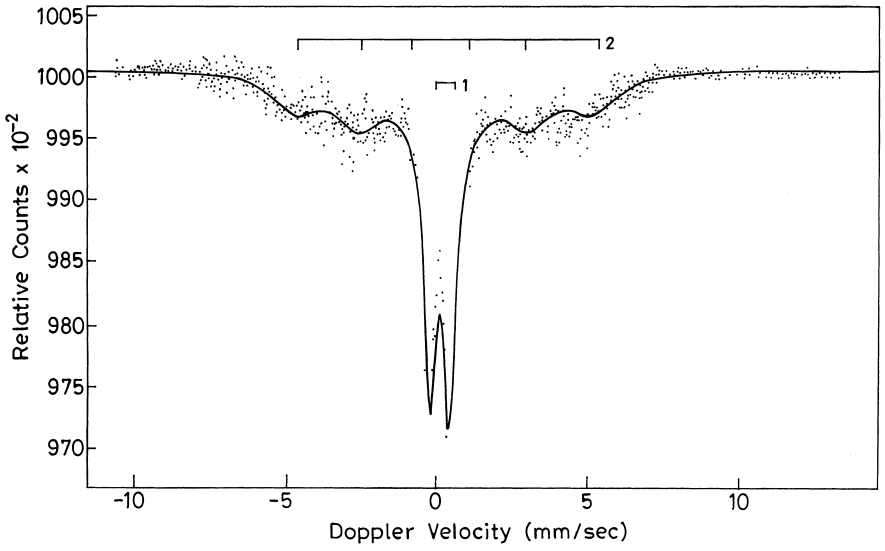

Fig. 8. Mössbauer spectrum obtained from the second DIP rust sample.

were 0.08 mm/s and 0.15 mm/s, it indicated the presence of magnetite in addition to the other species.

In both samples, an asymmetry of the right peak in the central doublet is observed which is generally not obtained. Meisel et al. [36], while studying rust conversion by phosphoric acid, noticed a singlet at about 0.42 mm/s, which was attributed to $FeH_3(PO_4)_2{\cdot}2.5H_2O$. The asymmetric second peak is also at 0.42 mm/s and this could be due to the merging of singlet along with the doublet due to other species. Therefore, Mössbauer spectroscopy also supports the XRD results obtained earlier, i.e. the identification of ferric hydrogen phosphate hydrate.

The rust from an ancient corrosion resistant Gupta period iron clamp has been earlier analyzed by Mössbauer spectroscopy [30]. Similar to the DIP rust, the Eran rust also showed a central doublet. Moreover, the Eran rust's central doublet exhibited asymmetry (larger intense left peak) which was due to the presence of ferrous phosphates. There was also a shoulder at more positive velocity region, which again confirmed that iron was in the ferrous state in the phosphate present in that rust [30]. In the case of the DIP rust, a similar asymmetry (i.e. higher intense left peak of central doublet) is absent (see Figs. 7 and 8) and there is no shoulder (in the positive velocity region). These observations clearly indicate that the iron in the phosphate is not in the ferrous state. This is an important result as this also indicates that the precursor phase (in which the iron is in the $+2$ oxidation state and also amorphous in nature [18]) to the crystalline iron hydrogen phosphate hydrate is absent in the DIP rust. This confirms the XRD results, which unambiguously concluded that the phosphate was crystalline iron hydrogen phosphate hydrate ($FeH_3P_2O_8{\cdot}4H_2O$ represented alternatively as $FePO_4{\cdot}H_3PO_4{\cdot}4H_2O$). In this phosphate, it can be clearly noticed that iron is in the ferric state.

4. Conclusions

The oldest rust from the DIP was characterized by XRD, FTIR and Mössbauer spectroscopy. XRD analyses confirmed the presence of crystalline hydrated iron hydrogen phosphate, i.e. $FeH_3P_2O_8{\cdot}4H_2O$ (which can also be viewed as $FePO_4{\cdot}H_3PO_4{\cdot}4H_2O$). The presence of a very small fraction of iron oxides/oxyhydroxides in the crystalline form was also indicated. The results of the FTIR study indicated that the constituents of the scale were γ-, α-, δ-FeOOH, magnetite and phosphate. The FTIR study also provided that the scale was hydrated. As XRD analysis did not reveal the presence of the hydrated iron oxides and oxyhydroxides, their identification in the FTIR spectrum implied that they are present in the amorphous state. Mössbauer spectroscopic analysis indicated that the rust contained γ-FeOOH, α-FeOOH, δ-FeOOH and magnetite in the amorphous form. This information was indirectly indicated by XRD, while the FTIR spectra could not provide this information. Therefore, Mössbauer spectroscopic study of the DIP rust confirms the amorphous nature of the

protective passive film, barring the phase iron hydrogen phosphate hydrate. The Mössbauer spectra also revealed that the iron in the crystalline iron hydrogen phosphate hydrate, whose presence was confirmed by XRD analysis, was in the ferric state.

Acknowledgements

The authors would like to thank the Archaeological Survey of India for permission to study the Delhi iron pillar and Director, Defense Materials and Stores Research and Development Establishment (DMSRDE), Kanpur for his co-operation.

References

[1] G. Wranglen, The rustless iron pillar at Delhi, Corrosion Science 10 (1970) 761–770.
[2] R. Balasubramaniam, Studies on the corrosion resistance of the Delhi iron pillar, NML Technical J. 37 (1995) 123–145.
[3] R. Balasubramaniam, Mixed potential theory analysis of the corrosion resistance of the Delhi iron pillar, Trans. Indian Inst. Metals 50 (1997) 23–35.
[4] D.A. Skoog, J.J. Leary, in: Principles of Instrumental Analysis, 4th ed., Harcourt Brace College Publishers, New York, 1992, pp. 252–309.
[5] T. Misawa, T. Kyuno, W. Suetaka, S. Shimodaira, The mechanism of atmospheric rusting and the effect of Cu and P on the rust formation of low alloy steels, Corrosion Science 11 (1971) 35–48.
[6] T. Misawa, K. Asami, K. Hashimoto, S. Shimodaira, The mechanism of atmospheric rusting and the protective amorphous rust on low alloy steel, Corrosion Science 14 (1974) 279–289.
[7] S. Music, M. Gotic, S. Popovic, X-ray diffraction and fourier transform infrared analysis of the rust formed by the corrosion of steel in aqueous solutions, J. Mater. Sci. 28 (1993) 5744–5751.
[8] A.K. Singh, R. Ericsson, L. Haggstrom, J. Gullman, Mössbauer and X-ray diffraction phases analysis of rusts from atmospheric test sites with different environments in Sweden, Corrosion Science 25 (1985) 931–945.
[9] T. Shinjo, Mössbauer effect in antiferromagnetic fine particles, J. Physical Society of Japan 21 (1966) 917–922.
[10] F. van der Woude, A.J. Dekker, Mössbauer Effect in α-FeOOH, Phys. Stat. Sol. 13 (1066) 181–193.
[11] M.J. Graham, M. Cohen, Analysis of iron corrosion products using Mössbauer spectroscopy, Corrosion 32 (1976) 432–438.
[12] H. Leidheiser Jr., I. Czako-Nagy, A Mössbauer spectroscopic study of rust formed during simulated atmospheric corrosion, Corrosion Science 24 (1984) 569–577.
[13] A. Vertes, I. Czako-Nagy, Mössbauer spectroscopy and its application to corrosion studies, Elctrochim. Acta 34 (1989) 721–758.
[14] J. Dannon, Fe: metals, alloys and inorganic compound, in: V.I. Goldanaskii, R.H. Herber (Eds.), Chemical applications of Mössbauer spectroscopy, Academic Press, New York, 1968, pp. 160–262.
[15] R. Balasubrmaniam, On the presence of lead in the Delhi iron pillar, Bull. Metals Museum 29-I (1998) 19–39.
[16] L. Bottyan, Gy. Fodag, K. Kulesar, D.L. Nagy, Central Research Institute of Physics, Budapest, Hungary.

[17] JCPDS Powder Diffraction Files, PCPDFWIN Software, Joint Committee on Powder Diffraction Standards — International Centre for Diffraction Data, Swarthmore, USA, 1996.
[18] E.L. Ghali, R.J.A. Potoin, The mechanism of phosphating of steel, Corrosion Science 12 (1972) 583–594.
[19] T.L. Woods, R.M. Garrels, in: Thermodynamic Values at Low Temperature for Natural Inorganic Materials, Oxford University Press, Oxford, 1987, pp. 100–106.
[20] V.A. Urasova, N.P. Levenets, A.M. Samarin, Non metallic inclusions in the Fe–P–O system, Izvest. Akad. Nauk SSSR, Metally 6 (1966) 24–30.
[21] W.E. Bardgett, J.F. Stanners, Delhi iron pillar — A study of the corrosion aspects, J. Iron and Steel Inst. 210 (1963) 3–10 and NML Technical J. 5 (1963) 24–30.
[22] M.K. Ghosh, The Delhi iron pillar and its iron, NML Technical J. 5 (1963) 31–45.
[23] A.K. Lahiri, T. Banerjee, B.R. Nijhawan, Some observations on corrosion-resistance of ancient Delhi iron pillar and present-time adivasi iron made by primitive methods, NML Tech. J. 5 (1963) 46–54.
[24] R. Balasubramaniam, On the corrosion resistance of the Delhi iron pillar, Corrosion Science, 42 (2000) 2103–2129.
[25] M. Ishii, M. Nakahira, Infrared absorption spectra and cation distributions in $(Mn,Fe)_3O_4$, Solid State Commn. 11 (1972) 209–212.
[26] A. Raman, B. Kuban, K. Razvan, The application of IR spectroscopy to the study of atmospheric rust systems: I standard spectra and illustrative applications to identify rust phases in natural corrosion, Corrosion Science 32 (1991) 1295–1306.
[27] M. Yamashita, H. Miyuki, Y. Matsuda, H. Nagano, T. Misawa, The long term growth of the protective rust layer formed on weathering steel by atmospheric corrosion during a quarter of a century, Corrosion Science 36 (1994) 283–299.
[28] R.A. Nyquist, R.A. Kagel (Eds.), IR Spectra of Inorganic Compounds, Academic Press, New York, 1971.
[29] J.M. Daniels, A. Rosenewaig, Mössbauer spectroscopy of stoichiometric and non-stoichiometric magnetite, J. Phys. Chem. Solids 30 (1969) 1561–1571.
[30] A.V. Ramesh Kumar, R. Balasubramaniam, Corrosion product analysis of ancient corrosion resistant Indian iron, Corrosion Science 40 (1998) 1169–1178.
[31] K.D. Bajpai, Coins from Eran excavations: a chronological analysis, in: D.W. Macdowall, S. Sharma, S. Garg (Eds.), Indian Numismatics: History, Art and Culture, vol. 1, Agam Kala Prakashan, New Delhi, 1990, pp. 79–92.
[32] R. Balasubramaniam, Identity of *Chandra* and *Vishnupadagiri* of the Delhi iron pillar inscription: numismatic, archaeological and literary evidence, Bull. Metals Museum 34 (2000) 42–64.
[33] A.N. Nigam, R.P. Tripathi, K. Dhoot, The effect of phosphoric acid on rust studied by Mössbauer spectroscopy, Corrosion Science 30 (1990) 799–803.
[34] M. Stratmann, K. Hoffman, In situ Mössbauer spectroscopic study of reaction with rust layers, Corrosion Science 29 (1989) 1329–1352.
[35] W. Kundig, H. Bommel, G. Constabalis, R.H. Lindquist, Some properties of supported small α-Fe_2O_3 particles determined with the Mössbauer effect, Physical Review 142 (1966) 327–333.
[36] W. Meisel, H.J. Guttmann, P. Gutlich, Influence of phosphoric acid on steel and on its corrosion products: a Mössbauer spectroscopic approach, Corrosion Science 23 (1983) 1373–1379.